Nonperturbative description of the butterfly diagram of energy spectra for materials immersed in a magnetic field

Katsuhiko Higuchi
Graduate School of Advanced Sciences of Matter, Hiroshima University, Higashi-Hiroshima 739-8527, Japan

Dipendra Bahadur Hamal
Department of Natural Sciences (Physics), Kathmandu University, Dhulikhel, Kavre 6250, Nepal

Masahiko Higuchi
Department of Physics, Faculty of Science, Shinshu University, Matsumoto 390-8621, Japan

(Received 22 February 2018; published 17 May 2018)

We propose a nonperturbative method to calculate the butterfly diagram of energy spectra for materials immersed in a magnetic field. We apply the proposed method to a crystalline silicon immersed in a magnetic field. It is shown that the conventional Hofstadter butterfly diagram is of low accuracy not only in the high magnetic field region of the diagram but also even in the experimentally available magnetic field region. This means that the present butterfly diagram is regarded as a replacement for the Hofstadter butterfly diagram. We also show that the correction to the Hofstadter buttery diagram would be observed under the ultrahigh magnetic field that is available in experiments.

DOI: 10.1103/PhysRevB.97.195135

I. INTRODUCTION

It is well known that the magnetic field dependence of energy levels of Bloch electrons in a magnetic field has a recursive structure [1]. Such a characteristic energy spectrum is referred to as the Hofstadter butterfly diagram and was first presented by Hofstadter [1]. The Hofstadter butterfly diagram has been effectively used for describing phenomena observed in a magnetic field. For example, it is shown that the characteristic gap structure of the Hofstadter butterfly diagram plays an essential role in the quantum Hall effect [2–4]. Besides this, de Haas–van Alphen (dHvA) oscillations and magnetic oscillations caused by magnetic breakdowns [5–12] can be described on the basis of the Hofstadter butterfly diagram. The direct observation of the Hofstadter butterfly diagram is done in the patterned AlGaAs/GaAs heterostructure [13,14], and also in the graphene/h-BN moiré superlattice [15–17].

We have recently developed the magnetic-field-containing relativistic tight-binding approximation (MFRTB) method that enables us to calculate the electronic structure of materials immersed in a magnetic field [18–21]. If the MFRTB method is applied to the two-dimensional square lattice with s electrons, then we get the relativistic version of the Hofstadter butterfly diagram, in which two butterfly diagrams overlap each other due to the Zeeman splitting of spin states [18]. If the Zeeman splitting of spin states is neglected, then the resultant energy spectrum coincides with the Hofstadter butterfly diagram [18]. We have also applied this method to a crystalline silicon. It was shown that nearly flat bands are obtained in the k_x-k_y plane of the magnetic first Brillouin zone [18]. This suggests that the motion of electrons in the plane perpendicular to the magnetic field is essentially changed corresponding to the quantization of the orbital motion of electrons in a magnetic field. It was also found that the magnetic field dependence of eigenvalues with wave vectors lying in the k_x-k_y plane exhibits the butterfly-like energy spectrum [18]. Furthermore, by means of the MFRTB method, we can not only revisit the dHvA oscillation and magnetic breakdown phenomena [19,20] but also predict additional oscillation peaks [21] of the magnetization that cannot be explained by the conventional Lifshitz-Kosevich formula [22].

Although the validity of the Hofstadter butterfly diagram has been confirmed as mentioned above, the confirmation is limited only to the low magnetic field region of the Hofstadter butterfly diagram. Note that the magnetic field used in experiments (up to about 45 T) corresponds to the low magnetic field region of the Hofstadter butterfly diagram. Furthermore, the Hofstadter butterfly diagram is recognized to be calculated within the lowest-order perturbation theory [18]. Therefore, it is expected that the Hofstadter butterfly diagram would be incorrect in the high magnetic field region or would be of low accuracy even in the low magnetic field region.

In this paper, we propose a method to calculate the butterfly diagram by means of the nonperturbative theory, which is hereafter referred to as the extended MFRTB (ext-MFRTB) method. In the ext-MFRTB method, the hopping integral in the presence of a magnetic field is described beyond the approximation of using the so-called Peierls phase factor [1,23] due to the nonperturbative theory. We apply the ext-MFRTB method to the crystalline silicon. It is shown that the discrepancy between the present butterfly diagram and the Hofstader one is caused by not only the anomalous Zeeman effect but also the Paschen-Back effect. In addition, we discuss the possibility of confirming the discrepancy experimentally by taking the recent progress of solid-state experiments under ultrahigh magnetic field [24–27] into consideration.

The outline of this paper is as follows. In Sec. II, we explain the reason why the nonperturbative method is needed for calculating the electronic structure of materials immersed in a magnetic field. In Sec. III, the ext-MFRTB method is proposed by using a nonperturbative method. It is shown that the application range of the ext-MFRTB method is extended from the low magnetic field to a high magnetic field region as compared with that of the Hofstadter and MFRTB methods. In Sec. IV, we apply the ext-MFRTB method to the crystalline silicon immersed in a magnetic field. It is shown that the butterfly diagram is much corrected by the ext-MFRTB method not only in the high magnetic field region but also in the low magnetic field region. In Sec. V, we give concluding remarks.

II. DIFFICULTY OF ADOPTING THE PERTURBATION THEORY FOR THE CALCULATION OF THE BUTTERFLY DIAGRAM

We first explain the difficulty of adopting the perturbation theory for the electronic structure calculations of materials immersed in a magnetic field. Let us start with the Dirac equation for an electron that moves in both a uniform magnetic field and periodic potential of the crystal:

$$\left[c\alpha\cdot\{\mathbf{p}+e\mathbf{A}(\mathbf{r})\}+\beta mc^2+\sum_n\sum_i v_{a_i}(\mathbf{r}-\mathbf{R}_n-\mathbf{d}_i)\right]\times\Phi_{\mathbf{k}}(\mathbf{r})=E(\mathbf{k})\Phi_{\mathbf{k}}(\mathbf{r}),\tag{1}$$

where $\mathbf{A}(\mathbf{r})$ and $v_{a_i}(\mathbf{r}-\mathbf{R}_n-\mathbf{d}_i)$ are the external vector potential of a uniform magnetic field $\mathbf{B}$ that is parallel to the z axis and scalar potential caused by the nucleus of atom a_i, respectively. Vectors $\mathbf{R}_n$ and $\mathbf{d}_i$ denote the translation vector of the lattice and vector specifying the position of atom a_i, respectively. In Eq. (1), c, e, and m denote the velocity of light, elementary charge, and rest mass of electrons, respectively, and the matrices $\alpha=(\alpha_x,\alpha_y,\alpha_z)$ and β stand for the usual 4×4 matrices. The subscript of $\Phi_{\mathbf{k}}(\mathbf{r})$ is the wave vector that belongs to the magnetic first Brillouin zone [18]. Suppose that the wave function $\Phi_{\mathbf{k}}(\mathbf{r})$ is expanded by means of relativistic atomic orbitals for atoms immersed in a uniform magnetic field. Namely, we have $\Phi_{\mathbf{k}}(\mathbf{r})=\sum_\xi\sum_n\sum_i C^\xi_{\mathbf{k}}(\mathbf{R}_n+\mathbf{d}_i)\psi_\xi^{a_i,\mathbf{R}_n+\mathbf{d}_i}(\mathbf{r})$, where $C^\xi_{\mathbf{k}}(\mathbf{R}_n+\mathbf{d}_i)$ is the expansion coefficient, and $\psi_\xi^{a_i,\mathbf{R}_n+\mathbf{d}_i}(\mathbf{r})$ denotes a relativistic atomic orbital for an atom a_i that is immersed in a uniform magnetic field and is located at $\mathbf{R}_n+\mathbf{d}_i$. By neglecting both overlap integrals involving different centers and hopping integrals involving three different centers, matrix elements of the Hamiltonian are given by [18]

$$\begin{aligned}&H_{\mathbf{R}_m j\eta,\mathbf{R}_n i\xi}\\&=\left(\varepsilon_\xi^{a_i,\mathbf{0}}+\Delta\varepsilon_\xi^{a_i,\mathbf{d}_i}\right)\delta_{\mathbf{R}_m,\mathbf{R}_n}\delta_{j,i}\delta_{\eta,\xi}+(1-\delta_{\mathbf{R}_m,\mathbf{R}_n}\delta_{j,i})\\&\quad\times e^{-i\frac{eB}{\hbar}(R_{nx}+d_{ix}-R_{mx}-d_{jx})(R_{my}+d_{jy})}\\&\quad\times T_{\eta\xi}^{a_j a_i}(\mathbf{R}_n-\mathbf{R}_m+\mathbf{d}_i-\mathbf{d}_j)\end{aligned}\tag{2}$$

with

$$\begin{aligned}&T_{\eta\xi}^{a_j a_i}(\mathbf{R}_l+\mathbf{d}_i-\mathbf{d}_j)\\&=\int\psi_\eta^{a_j,\mathbf{0}}(\mathbf{r})^\dagger\frac{v_{a_j}(\mathbf{r})+v_{a_i}(\mathbf{r}-\mathbf{R}_l-\mathbf{d}_i+\mathbf{d}_j)}{2}\\&\quad\times\psi_\xi^{a_i,\mathbf{R}_l+\mathbf{d}_i-\mathbf{d}_j}(\mathbf{r})d^3r,\end{aligned}\tag{3}$$

where $T_{\eta\xi}^{a_j a_i}$, $\varepsilon_\xi^{a_i,\mathbf{0}}$, and $\Delta\varepsilon_\xi^{a_i,\mathbf{d}_i}$ denote the hopping integral, atomic spectrum, and energy of the crystal field in the presence of a magnetic field, respectively. Hereafter, $T_{\eta\xi}^{a_j a_i}$ is referred to as the magnetic hopping integral.

In order to clarify the difficulty of using the perturbation theory, we hereafter give approximate forms of $T_{\eta\xi}^{a_j a_i}$ and $\varepsilon_\xi^{a_i,\mathbf{0}}$ that are obtained by the perturbation theory. Let us consider the Dirac equation for an isolated atom that is located at the origin and is immersed in a uniform magnetic field:

$$\left[c\alpha\cdot\{\mathbf{p}+e\mathbf{A}(\mathbf{r})\}+\beta mc^2+v_{a_i}(\mathbf{r})\right]\psi_\xi^{a_i,\mathbf{0}}(\mathbf{r})=\varepsilon_\xi^{a_i,\mathbf{0}}\psi_\xi^{a_i,\mathbf{0}}(\mathbf{r}).\tag{4}$$

If the effect of the magnetic field, $ec\alpha\cdot\mathbf{A}(\mathbf{r})$, is treated as the perturbation, then we can derive the perturbation corrections for the unperturbed eigenvalue $\bar\varepsilon_{nlJ}^{a_i}$ and eigenfunction $\phi_{n\ell JM}^{a_i}(\mathbf{r})$, where subscripts n, l, J, and M are the principal, azimuthal, total angular momentum, and magnetic quantum numbers, respectively. Specifically, within the second-order perturbation theory, we have

$$\begin{aligned}\varepsilon_\xi^{a_i,\mathbf{0}}=\bar\varepsilon_{nlJ}^{a_i}+\frac{e\hbar B}{2m}\Bigg\{&\frac{2J+1}{2l+1}M+\frac{\lambda_{lM}}{(2l+1)^2}S_{nlJ}^2x_{nl}\\&-\frac{2\lambda_{lM}M}{(2l+1)^3}S_{nlJ}^2x_{nl}^2\Bigg\},\end{aligned}\tag{5}$$

$$\begin{aligned}\psi_\xi^{a_i,\mathbf{0}}(\mathbf{r})=\phi_{n\ell JM}^{a_i}(\mathbf{r})&\pm\frac{\sqrt{\lambda_{lM}}}{2l+1}S_{nlJ}\\&\times\left(x_{nl}+\frac{M}{l+1/2}x_{nl}^2\right)\phi_{n\ell J\mp1M}^{a_i}(\mathbf{r})\end{aligned}\tag{6}$$

with

$$x_{nl}=\left.\frac{e\hbar B/2m}{\bar\varepsilon_{nlJ}^{a_i}-\bar\varepsilon_{nlJ-1}^{a_i}}\right|_{J=l+1/2}\tag{7}$$

for the case of $J=l\pm1/2$. Here $\lambda_{lM}=(l+1/2-M)(l+1/2+M)$, and S_{nlJ} denotes the overlap integral between the radial parts of $\phi_{n\ell JM}^{a_i}(\mathbf{r})$ and $\phi_{n\ell J-1M}^{a_i}(\mathbf{r})$. In Eq. (7), x_{nl} is defined as the ratio of $e\hbar B/2m$ that represents the extent of the Zeeman splitting to $\bar\varepsilon_{nlJ}^{a_i}-\bar\varepsilon_{nlJ-1}^{a_i}$ that represents the spin-orbit splitting.

If the zeroth-order approximation is adopted for both the eigenvalue and eigenfunction, then we have $\varepsilon_\xi^{a_i,\mathbf{0}}\sim\bar\varepsilon_{nlJ}^{a_i}$ and $\psi_\xi^{a_i,\mathbf{0}}(\mathbf{r})\sim\phi_{n\ell JM}^{a_i}(\mathbf{r})$. This zeroth-order approximation leads to the butterfly diagram that is the same as the Hofstadter one for the two-dimensional square lattice model with s electrons [18]. On the other hand, the first-order correction for the eigenvalue is taken into account in the MFRTB method [18]; i.e., the eigenvalue is approximated by

$$\varepsilon_\xi^{a_i,\mathbf{0}}=\bar\varepsilon_{nlJ}^{a_i}+\left(\frac{e\hbar B}{2m}\right)\frac{2J+1}{2l+1}M.\tag{8}$$

Here note that the correction term just corresponds to the anomalous Zeeman effect. Since the eigenfunction is approximated within the zeroth order in the MFRTB method as well as in the Hofstadter method, the magnetic hopping integral can be approximated by

$$T_{n'l'J'M',nlJM}^{a_j a_i}(\mathbf{R})=e^{-i\frac{eB}{2\hbar}R_xR_y}t_{n'l'J'M',nlJM}^{a_j a_i}(\mathbf{R}),\tag{9}$$

where R_x and R_y denote the x and y components of $\mathbf{R}$, respectively, and $t^{a_j a_i}_{n'l'J'M',nlJM}(\mathbf{R})$ denotes a hopping integral in the absence of a magnetic field. The hopping integral $t^{a_j a_i}_{n'l'J'M',nlJM}(\mathbf{R})$ can be calculated by means of the relativistic version of the so-called Slater-Koster table [18]. It should be noted that Eq. (9) corresponds to the well-known approximation of using the Peierls phase factor [1,23]. Equation (9) is widely used as the approximation of the magnetic hopping integral [23].

It is noticed from Eqs. (5) and (6) that perturbation correction terms for the eigenvalue and eigenfunction are expressed in terms of power series of x_{nl} that is defined by Eq. (7). This means that the perturbation theory becomes invalid in the high magnetic field region such that $x_{nl} > 1$. Therefore, we can say that the correctness of the Hofstadter butterfly diagram gets worse with increasing magnetic field. For example, the spin-orbit splittings of p states for C and Si are about 0.0083 eV and 0.0294 eV, respectively[28]. Therefore, the magnetic fields that satisfy $x_{nl} = 1$ are about 144 T and 509 T for C and Si, respectively. Since the recent progress of the electromagnetic flux compression method enables one to perform solid-state experiments in the ultrahigh magnetic field up to 730 T [24–27], it is expected that the failure or incorrectness of the Hofstadter butterfly diagram would be observed by experiments.

III. EXTENDED MFRTB METHOD

In order to avoid the above-mentioned difficulty of the perturbation theory, $T^{a_j a_i}_{n\xi}$ and $\varepsilon^{a_i,\mathbf{0}}_{\xi}$ are evaluated by means of the nonperturbative method in the ext-MFRTB method. Specifically, we consider matrix elements of the Hamiltonian of Eq. (4) by using atomic orbitals in the absence of a magnetic field [i.e., $\phi^{a_i}_{n\ell JM}(\mathbf{r})$] as basis functions. In the derivation of matrix elements, only the outermost atomic orbitals are taken into consideration, and the small component of $\phi^{a_i}_{n\ell JM}(\mathbf{r})$ is approximated by $g^{a_i}_{nlJM}(\mathbf{r}) \approx \sigma \cdot \mathbf{p}\, f^{a_i}_{nlJM}(\mathbf{r})/2mc$, where σ, $f^{a_i}_{nlJM}(\mathbf{r})$, and $g^{a_i}_{nlJM}(\mathbf{r})$ denote the Pauli matrix and the large and small components of $\phi^{a_i}_{n\ell JM}(\mathbf{r})$, respectively [29]. By diagonalizing the resultant matrix, we obtain the eigenvalues and eigenfunctions that correspond to unperturbed atomic states (n, l, J, M) and $(n, l, J-1, M)$ with $J = l + 1/2$ and $M \neq \pm J$:

$$\varepsilon^{a_i,\mathbf{0}}_{\xi} = \frac{\bar{\varepsilon}^{a_i}_{nlJ} + \bar{\varepsilon}^{a_i}_{nlJ-1}}{2} + \frac{e\hbar B}{2m} M \pm \frac{\bar{\varepsilon}^{a_i}_{nlJ} - \bar{\varepsilon}^{a_i}_{nlJ-1}}{2} \sqrt{1 + 2\frac{M}{J} x_{nl} + \frac{(J^2 - M^2)S^2_{nlJ} + M^2}{J^2} x^2_{nl}}, \tag{10}$$

$$\psi^{a_i\xi}_{\mathbf{0}}(\mathbf{r}) = \begin{cases} \dfrac{\varphi^{a_i}_{nlJM}(\mathbf{r}) + \eta^{a_i}_{nlJM}\varphi^{a_i}_{nlJ-1M}(\mathbf{r})}{\sqrt{1 + \left(\eta^{a_i}_{nlJM}\right)^2}} & \text{for } (n,l,J,M),\ M \neq \pm J, \\ \dfrac{\varphi^{a_i}_{nlJ-1M}(\mathbf{r}) + \eta^{a_i}_{nlJ-1M}\varphi^{a_i}_{nlJM}(\mathbf{r})}{\sqrt{1 + \left(\eta^{a_i}_{nlJ-1M}\right)^2}} & \text{for } (n,l,J-1,M), \end{cases} \tag{11}$$

$$\eta^{a_i}_{nlJM} = -\eta^{a_i}_{nlJ-1M} = \frac{J}{S_{nlJ}(J^2 - M^2)x_{nl}} \left\{ 1 + \frac{M}{J} x_{nl} - \sqrt{1 + 2\frac{M}{J} x_{nl} + \frac{(J^2 - M^2)S^2_{nlJ} + M^2}{J^2} x^2_{nl}} \right\}, \tag{12}$$

where the upper and lower signs in Eq. (10) correspond to (n, l, J, M) and $(n, l, J-1, M)$, respectively. Concerning the eigenvalues and eigenfunctions that correspond to unperturbed atomic states $(n, l, J, \pm J)$ with $J = l + 1/2$, we have

$$\varepsilon^{a_i,\mathbf{0}}_{\xi} = \bar{\varepsilon}^{a_i}_{nlJ} \pm \frac{e\hbar B}{4m}(2J + 1), \tag{13}$$

$$\psi^{a_i\xi}_{\mathbf{0}}(\mathbf{r}) = \varphi^{a_i}_{nlJ\pm J}(\mathbf{r}). \tag{14}$$

Substituting Eqs. (11) and/or (14) into Eq. (3), we can get the approximate form of the magnetic hopping integral. In the cases of $l = 0$ and 1, the resultant expressions are summarized in Table I. Since the mixing coefficient $\eta^{a_i}_{nlJM}$ approaches zero in the limit of the low magnetic field, approximate forms listed in Table I coincide with Eq. (9) in the limit of the low magnetic field. Therefore, we can say that approximate forms listed in Table I are regarded as the correction to Eq. (9) that just corresponds to the approximation of using the Peierls phase factor [1,23].

It can be confirmed that Eqs. (10)–(14) are reduced to results of the perturbation theory in the case of $x_{nl} \ll 1$. This means that Eqs. (10)–(14) include the corresponding expressions based on the perturbation theory in the case of the low magnetic field. Furthermore, Eq. (10) is approximated by $(\bar{\varepsilon}^{a_i}_{nlJ} + \bar{\varepsilon}^{a_i}_{nlJ-1})/2 + (e\hbar B/2m)(M \pm 1/2)$ in the case of $x_{nl} \gg 1$ (high magnetic field case). The second terms of this expression and Eq. (13) just correspond to the energy shift of the Paschen-Back effect [30]. Therefore, Eqs. (10) and (13) and the magnetic hopping integrals listed in Table I are recognized as the corrected expressions that include not only the Zeeman effect but also the Paschen-Back effect.

We can extend the applicable range of the MFRTB method from the low magnetic field region ($x_{nl} \ll 1$) to the high magnetic field region ($x_{nl} \gg 1$) if we adopt Eqs. (10) and (13) and Table I as $\varepsilon^{a_i,\mathbf{0}}_{\xi}$ and $T^{a_j a_i}_{n'l'J'M',nlJM}$. Thus, the present method, which is referred to as the ext-MFRTB method, enables us to obtain the butterfly diagram that includes not only the Zeeman

TABLE I. Magnetic hopping integrals $T^{a_j,a_i}_{nl'J'M',nlJM}(\mathbf{R})$ calculated by using Eqs. (11) and (14). In this table, η_α and η_β are defined by $\eta_\alpha = \eta^{a_i}_{n1\frac{3}{2}\frac{1}{2}} = -\eta^{a_i}_{n1\frac{1}{2}\frac{1}{2}}$ and $\eta_\beta = \eta^{a_i}_{n1\frac{3}{2}-\frac{1}{2}} = -\eta^{a_i}_{n1\frac{1}{2}-\frac{1}{2}}$, respectively. Here, note that $t^{a_j,a_i}_{nl'J'M',nlJM}(\mathbf{R})$ can be calculated by means of the relativistic version of the Slater-Koster table [18].

(n,l',J',M')	(n,l,J,M)	Hopping integrals $T^{a_j,a_i}_{nl'J'M',nlJM}(\mathbf{R})$
$(n,0,\frac{1}{2},\frac{1}{2})$	$(n,0,\frac{1}{2},\frac{1}{2})$	$e^{-i\frac{eB}{2\hbar}R_xR_y}t^{a_j,a_i}_{n0\frac{1}{2}\frac{1}{2},n0\frac{1}{2}\frac{1}{2}}(\mathbf{R})$
$(n,0,\frac{1}{2},\frac{1}{2})$	$(n,0,\frac{1}{2},-\frac{1}{2})$	$e^{-i\frac{eB}{2\hbar}R_xR_y}t^{a_j,a_i}_{n0\frac{1}{2}\frac{1}{2},n0\frac{1}{2}\frac{-1}{2}}(\mathbf{R})$
$(n,0,\frac{1}{2},\frac{1}{2})$	$(n,1,\frac{1}{2},\frac{1}{2})$	$e^{-i\frac{eB}{2\hbar}R_xR_y}\{t^{a_j,a_i}_{n0\frac{1}{2}\frac{1}{2},n1\frac{1}{2}\frac{1}{2}}(\mathbf{R})-\eta_\alpha t^{a_j,a_i}_{n0\frac{1}{2}\frac{1}{2},n1\frac{3}{2}\frac{1}{2}}(\mathbf{R})\}/\sqrt{1+\eta_\alpha^2}$
$(n,0,\frac{1}{2},\frac{1}{2})$	$(n,1,\frac{1}{2},-\frac{1}{2})$	$e^{-i\frac{eB}{2\hbar}R_xR_y}\{t^{a_j,a_i}_{n0\frac{1}{2}\frac{1}{2},n1\frac{1}{2}\frac{-1}{2}}(\mathbf{R})-\eta_\beta t^{a_j,a_i}_{n0\frac{1}{2}\frac{1}{2},n1\frac{3}{2}\frac{-1}{2}}(\mathbf{R})\}/\sqrt{1+\eta_\beta^2}$
$(n,0,\frac{1}{2},\frac{1}{2})$	$(n,1,\frac{3}{2},\frac{3}{2})$	$e^{-i\frac{eB}{2\hbar}R_xR_y}t^{a_j,a_i}_{n0\frac{1}{2}\frac{1}{2},n1\frac{3}{2}\frac{3}{2}}(\mathbf{R})$
$(n,0,\frac{1}{2},\frac{1}{2})$	$(n,1,\frac{3}{2},\frac{1}{2})$	$e^{-i\frac{eB}{2\hbar}R_xR_y}\{t^{a_j,a_i}_{n0\frac{1}{2}\frac{1}{2},n1\frac{3}{2}\frac{1}{2}}(\mathbf{R})+\eta_\alpha t^{a_j,a_i}_{n0\frac{1}{2}\frac{1}{2},n1\frac{1}{2}\frac{1}{2}}(\mathbf{R})\}/\sqrt{1+\eta_\alpha^2}$
$(n,0,\frac{1}{2},\frac{1}{2})$	$(n,1,\frac{3}{2},-\frac{1}{2})$	$e^{-i\frac{eB}{2\hbar}R_xR_y}\{t^{a_j,a_i}_{n0\frac{1}{2}\frac{1}{2},n1\frac{3}{2}\frac{-1}{2}}(\mathbf{R})+\eta_\beta t^{a_j,a_i}_{n0\frac{1}{2}\frac{1}{2},n1\frac{1}{2}\frac{-1}{2}}(\mathbf{R})\}/\sqrt{1+\eta_\beta^2}$
$(n,0,\frac{1}{2},\frac{1}{2})$	$(n,1,\frac{3}{2},-\frac{3}{2})$	$e^{-i\frac{eB}{2\hbar}R_xR_y}t^{a_j,a_i}_{n0\frac{1}{2}\frac{1}{2},n1\frac{3}{2}\frac{-3}{2}}(\mathbf{R})$
$(n,0,\frac{1}{2},-\frac{1}{2})$	$(n,0,\frac{1}{2},\frac{1}{2})$	$e^{-i\frac{eB}{2\hbar}R_xR_y}t^{a_j,a_i}_{n0\frac{1}{2}\frac{-1}{2},n0\frac{1}{2}\frac{1}{2}}(\mathbf{R})$
$(n,0,\frac{1}{2},-\frac{1}{2})$	$(n,0,\frac{1}{2},-\frac{1}{2})$	$e^{-i\frac{eB}{2\hbar}R_xR_y}t^{a_j,a_i}_{n0\frac{1}{2}\frac{-1}{2},n0\frac{1}{2}\frac{-1}{2}}(\mathbf{R})$
$(n,0,\frac{1}{2},-\frac{1}{2})$	$(n,1,\frac{1}{2},\frac{1}{2})$	$e^{-i\frac{eB}{2\hbar}R_xR_y}\{t^{a_j,a_i}_{n0\frac{1}{2}\frac{-1}{2},n1\frac{1}{2}\frac{1}{2}}(\mathbf{R})-\eta_\alpha t^{a_j,a_i}_{n0\frac{1}{2}\frac{-1}{2},n1\frac{3}{2}\frac{1}{2}}(\mathbf{R})\}/\sqrt{1+\eta_\alpha^2}$
$(n,0,\frac{1}{2},-\frac{1}{2})$	$(n,1,\frac{1}{2},\frac{1}{2})$	$e^{-i\frac{eB}{2\hbar}R_xR_y}\{t^{a_j,a_i}_{n0\frac{1}{2}\frac{-1}{2},n1\frac{1}{2}\frac{-1}{2}}(\mathbf{R})-\eta_\beta t^{a_j,a_i}_{n0\frac{1}{2}\frac{-1}{2},n1\frac{3}{2}\frac{-1}{2}}(\mathbf{R})\}/\sqrt{1+\eta_\beta^2}$
$(n,0,\frac{1}{2},-\frac{1}{2})$	$(n,1,\frac{3}{2},\frac{3}{2})$	$e^{-i\frac{eB}{2\hbar}R_xR_y}t^{a_j,a_i}_{n0\frac{1}{2}\frac{-1}{2},n1\frac{3}{2}\frac{3}{2}}(\mathbf{R})$
$(n,0,\frac{1}{2},-\frac{1}{2})$	$(n,1,\frac{3}{2},\frac{1}{2})$	$e^{-i\frac{eB}{2\hbar}R_xR_y}\{t^{a_j,a_i}_{n0\frac{1}{2}\frac{-1}{2},n1\frac{3}{2}\frac{1}{2}}(\mathbf{R})+\eta_\alpha t^{a_j,a_i}_{n0\frac{1}{2}\frac{-1}{2},n1\frac{1}{2}\frac{1}{2}}(\mathbf{R})\}/\sqrt{1+\eta_\alpha^2}$
$(n,0,\frac{1}{2},-\frac{1}{2})$	$(n,1,\frac{3}{2},-\frac{1}{2})$	$e^{-i\frac{eB}{2\hbar}R_xR_y}\{t^{a_j,a_i}_{n0\frac{1}{2}\frac{-1}{2},n1\frac{3}{2}\frac{-1}{2}}(\mathbf{R})+\eta_\beta t^{a_j,a_i}_{n0\frac{1}{2}\frac{-1}{2},n1\frac{1}{2}\frac{-1}{2}}(\mathbf{R})\}/\sqrt{1+\eta_\beta^2}$
$(n,0,\frac{1}{2},-\frac{1}{2})$	$(n,1,\frac{3}{2},-\frac{3}{2})$	$e^{-i\frac{eB}{2\hbar}R_xR_y}t^{a_j,a_i}_{n0\frac{1}{2}\frac{-1}{2},n1\frac{3}{2}\frac{-3}{2}}(\mathbf{R})$
$(n,1,\frac{1}{2},\frac{1}{2})$	$(n,0,\frac{1}{2},\frac{1}{2})$	$e^{-i\frac{eB}{2\hbar}R_xR_y}\{t^{a_j,a_i}_{n1\frac{1}{2}\frac{1}{2},n0\frac{1}{2}\frac{1}{2}}(\mathbf{R})-\eta_\alpha t^{a_j,a_i}_{n1\frac{3}{2}\frac{1}{2},n0\frac{1}{2}\frac{1}{2}}(\mathbf{R})\}/\sqrt{1+\eta_\alpha^2}$
$(n,1,\frac{1}{2},\frac{1}{2})$	$(n,0,\frac{1}{2},-\frac{1}{2})$	$e^{-i\frac{eB}{2\hbar}R_xR_y}\{t^{a_j,a_i}_{n1\frac{1}{2}\frac{1}{2},n0\frac{1}{2}\frac{-1}{2}}(\mathbf{R})-\eta_\alpha t^{a_j,a_i}_{n1\frac{3}{2}\frac{1}{2},n0\frac{1}{2}\frac{-1}{2}}(\mathbf{R})\}/\sqrt{1+\eta_\alpha^2}$
$(n,1,\frac{1}{2},\frac{1}{2})$	$(n,1,\frac{1}{2},\frac{1}{2})$	$e^{-i\frac{eB}{2\hbar}R_xR_y}\{t^{a_j,a_i}_{n1\frac{1}{2}\frac{1}{2},n1\frac{1}{2}\frac{1}{2}}(\mathbf{R})-\eta_\alpha t^{a_j,a_i}_{n1\frac{3}{2}\frac{1}{2},n1\frac{1}{2}\frac{1}{2}}(\mathbf{R})$ $-\eta_\alpha t^{a_j,a_i}_{n1\frac{1}{2}\frac{1}{2},n1\frac{3}{2}\frac{1}{2}}(\mathbf{R})+\eta_\alpha^2 t^{a_j,a_i}_{n1\frac{3}{2}\frac{1}{2},n1\frac{3}{2}\frac{1}{2}}(\mathbf{R})\}/(1+\eta_\alpha^2)$
$(n,1,\frac{1}{2},\frac{1}{2})$	$(n,1,\frac{1}{2},-\frac{1}{2})$	$e^{-i\frac{eB}{2\hbar}R_xR_y}\{t^{a_j,a_i}_{n1\frac{1}{2}\frac{1}{2},n1\frac{1}{2}\frac{-1}{2}}(\mathbf{R})-\eta_\alpha t^{a_j,a_i}_{n1\frac{3}{2}\frac{1}{2},n1\frac{1}{2}\frac{-1}{2}}(\mathbf{R})$ $-\eta_\beta t^{a_j,a_i}_{n1\frac{1}{2}\frac{1}{2},n1\frac{3}{2}\frac{-1}{2}}(\mathbf{R})+\eta_\alpha\eta_\beta t^{a_j,a_i}_{n1\frac{3}{2}\frac{1}{2},n1\frac{3}{2}\frac{-1}{2}}(\mathbf{R})\}/\sqrt{(1+\eta_\alpha^2)(1+\eta_\beta^2)}$
$(n,1,\frac{1}{2},\frac{1}{2})$	$(n,1,\frac{3}{2},\frac{3}{2})$	$e^{-i\frac{eB}{2\hbar}R_xR_y}\{t^{a_j,a_i}_{n1\frac{1}{2}\frac{1}{2},n1\frac{3}{2}\frac{3}{2}}(\mathbf{R})-\eta_\alpha t^{a_j,a_i}_{n1\frac{3}{2}\frac{1}{2},n1\frac{3}{2}\frac{3}{2}}(\mathbf{R})\}/\sqrt{1+\eta_\alpha^2}$
$(n,1,\frac{1}{2},\frac{1}{2})$	$(n,1,\frac{3}{2},\frac{1}{2})$	$e^{-i\frac{eB}{2\hbar}R_xR_y}\{t^{a_j,a_i}_{n1\frac{1}{2}\frac{1}{2},n1\frac{3}{2}\frac{1}{2}}(\mathbf{R})-\eta_\alpha t^{a_j,a_i}_{n1\frac{3}{2}\frac{1}{2},n1\frac{3}{2}\frac{1}{2}}(\mathbf{R})$ $+\eta_\alpha t^{a_j,a_i}_{n1\frac{1}{2}\frac{1}{2},n1\frac{1}{2}\frac{1}{2}}(\mathbf{R})-\eta_\alpha^2 t^{a_j,a_i}_{n1\frac{3}{2}\frac{1}{2},n1\frac{1}{2}\frac{1}{2}}(\mathbf{R})\}/(1+\eta_\alpha^2)$
$(n,1,\frac{1}{2},\frac{1}{2})$	$(n,1,\frac{3}{2},-\frac{1}{2})$	$e^{-i\frac{eB}{2\hbar}R_xR_y}\{t^{a_j,a_i}_{n1\frac{1}{2}\frac{1}{2},n1\frac{3}{2}\frac{-1}{2}}(\mathbf{R})-\eta_\alpha t^{a_j,a_i}_{n1\frac{3}{2}\frac{1}{2},n1\frac{3}{2}\frac{-1}{2}}(\mathbf{R})$ $+\eta_\beta t^{a_j,a_i}_{n1\frac{1}{2}\frac{1}{2},n1\frac{1}{2}\frac{-1}{2}}(\mathbf{R})-\eta_\alpha\eta_\beta t^{a_j,a_i}_{n1\frac{3}{2}\frac{1}{2},n1\frac{1}{2}\frac{-1}{2}}(\mathbf{R})\}/\sqrt{(1+\eta_\alpha^2)(1+\eta_\beta^2)}$
$(n,1,\frac{1}{2},\frac{1}{2})$	$(n,1,\frac{3}{2},-\frac{3}{2})$	$e^{-i\frac{eB}{2\hbar}R_xR_y}\{t^{a_j,a_i}_{n1\frac{1}{2}\frac{1}{2},n1\frac{3}{2}\frac{-3}{2}}(\mathbf{R})-\eta_\alpha t^{a_j,a_i}_{n1\frac{3}{2}\frac{1}{2},n1\frac{3}{2}\frac{-3}{2}}(\mathbf{R})\}/\sqrt{1+\eta_\alpha^2}$
$(n,1,\frac{1}{2},-\frac{1}{2})$	$(n,0,\frac{1}{2},\frac{1}{2})$	$e^{-i\frac{eB}{2\hbar}R_xR_y}\{t^{a_j,a_i}_{n1\frac{1}{2}\frac{-1}{2},n0\frac{1}{2}\frac{1}{2}}(\mathbf{R})-\eta_\beta t^{a_j,a_i}_{n1\frac{3}{2}\frac{-1}{2},n0\frac{1}{2}\frac{1}{2}}(\mathbf{R})\}/\sqrt{1+\eta_\beta^2}$
$(n,1,\frac{1}{2},-\frac{1}{2})$	$(n,0,\frac{1}{2},-\frac{1}{2})$	$e^{-i\frac{eB}{2\hbar}R_xR_y}\{t^{a_j,a_i}_{n1\frac{1}{2}\frac{-1}{2},n0\frac{1}{2}\frac{-1}{2}}(\mathbf{R})-\eta_\beta t^{a_j,a_i}_{n1\frac{3}{2}\frac{-1}{2},n0\frac{1}{2}\frac{-1}{2}}(\mathbf{R})\}/\sqrt{1+\eta_\beta^2}$

TABLE I. (*Continued*.)

(n,l',J',M')	(n,l,J,M)	Hopping integrals $T^{a_j,a_i}_{nl'J'M',nlJM}(\mathbf{R})$
$(n,1,\frac{1}{2},-\frac{1}{2})$	$(n,1,\frac{1}{2},\frac{1}{2})$	$e^{-i\frac{eB}{2\hbar}R_xR_y}\{t^{a_j,a_i}_{n1\frac{1}{2}\frac{-1}{2},n1\frac{1}{2}\frac{1}{2}}(\mathbf{R})-\eta_\beta t^{a_j,a_i}_{n1\frac{1}{2}\frac{-1}{2},n1\frac{3}{2}\frac{1}{2}}(\mathbf{R})$ $-\eta_\alpha t^{a_j,a_i}_{n1\frac{1}{2}\frac{-1}{2},n1\frac{3}{2}\frac{1}{2}}(\mathbf{R})+\eta_\alpha\eta_\beta t^{a_j,a_i}_{n1\frac{3}{2}\frac{-1}{2},n1\frac{3}{2}\frac{1}{2}}(\mathbf{R})\}/\sqrt{(1+\eta_\alpha^2)(1+\eta_\beta^2)}$
$(n,1,\frac{1}{2},-\frac{1}{2})$	$(n,1,\frac{1}{2},-\frac{1}{2})$	$e^{-i\frac{eB}{2\hbar}R_xR_y}\{t^{a_j,a_i}_{n1\frac{1}{2}\frac{-1}{2},n1\frac{1}{2}\frac{-1}{2}}(\mathbf{R})-\eta_\beta t^{a_j,a_i}_{n1\frac{3}{2}\frac{-1}{2},n1\frac{1}{2}\frac{-1}{2}}(\mathbf{R})$ $-\eta_\beta t^{a_j,a_i}_{n1\frac{1}{2}\frac{-1}{2},n1\frac{3}{2}\frac{-1}{2}}(\mathbf{R})+\eta_\beta^2 t^{a_j,a_i}_{n1\frac{3}{2}\frac{-1}{2},n1\frac{3}{2}\frac{-1}{2}}(\mathbf{R})\}/(1+\eta_\beta^2)$
$(n,1,\frac{1}{2},-\frac{1}{2})$	$(n,1,\frac{3}{2},\frac{3}{2})$	$e^{-i\frac{eB}{2\hbar}R_xR_y}\{t^{a_j,a_i}_{n1\frac{1}{2}\frac{-1}{2},n1\frac{3}{2}\frac{3}{2}}(\mathbf{R})-\eta_\beta t^{a_j,a_i}_{n1\frac{3}{2}\frac{-1}{2},n1\frac{3}{2}\frac{3}{2}}(\mathbf{R})\}/\sqrt{1+\eta_\beta^2}$
$(n,1,\frac{1}{2},-\frac{1}{2})$	$(n,1,\frac{3}{2},\frac{1}{2})$	$e^{-i\frac{eB}{2\hbar}R_xR_y}\{t^{a_j,a_i}_{n1\frac{1}{2}\frac{-1}{2},n1\frac{3}{2}\frac{1}{2}}(\mathbf{R})-\eta_\beta t^{a_j,a_i}_{n1\frac{3}{2}\frac{-1}{2},n1\frac{3}{2}\frac{1}{2}}(\mathbf{R})$ $+\eta_\alpha t^{a_j,a_i}_{n1\frac{1}{2}\frac{-1}{2},n1\frac{1}{2}\frac{1}{2}}(\mathbf{R})-\eta_\alpha\eta_\beta t^{a_j,a_i}_{n1\frac{3}{2}\frac{-1}{2},n1\frac{1}{2}\frac{1}{2}}(\mathbf{R})\}/\sqrt{(1+\eta_\alpha^2)(1+\eta_\beta^2)}$
$(n,1,\frac{1}{2},-\frac{1}{2})$	$(n,1,\frac{3}{2},-\frac{1}{2})$	$e^{-i\frac{eB}{2\hbar}R_xR_y}\{t^{a_j,a_i}_{n1\frac{1}{2}\frac{-1}{2},n1\frac{3}{2}\frac{-1}{2}}(\mathbf{R})-\eta_\beta t^{a_j,a_i}_{n1\frac{3}{2}\frac{-1}{2},n1\frac{3}{2}\frac{-1}{2}}(\mathbf{R})$ $+\eta_\beta t^{a_j,a_i}_{n1\frac{1}{2}\frac{-1}{2},n1\frac{1}{2}\frac{-1}{2}}(\mathbf{R})-\eta_\beta^2 t^{a_j,a_i}_{n1\frac{3}{2}\frac{-1}{2},n1\frac{1}{2}\frac{-1}{2}}(\mathbf{R})\}/(1+\eta_\beta^2)$
$(n,1,\frac{1}{2},-\frac{1}{2})$	$(n,1,\frac{3}{2},-\frac{3}{2})$	$e^{-i\frac{eB}{2\hbar}R_xR_y}\{t^{a_j,a_i}_{n1\frac{1}{2}\frac{-1}{2},n1\frac{3}{2}\frac{-3}{2}}(\mathbf{R})-\eta_\beta t^{a_j,a_i}_{n1\frac{3}{2}\frac{-1}{2},n1\frac{3}{2}\frac{-3}{2}}(\mathbf{R})\}/\sqrt{1+\eta_\beta^2}$
$(n,1,\frac{3}{2},\frac{3}{2})$	$(n,0,\frac{1}{2},\frac{1}{2})$	$e^{-i\frac{eB}{2\hbar}R_xR_y}t^{a_j,a_i}_{n1\frac{3}{2}\frac{3}{2},n0\frac{1}{2}\frac{1}{2}}(\mathbf{R})$
$(n,1,\frac{3}{2},\frac{3}{2})$	$(n,0,\frac{1}{2},-\frac{1}{2})$	$e^{-i\frac{eB}{2\hbar}R_xR_y}t^{a_j,a_i}_{n1\frac{3}{2}\frac{3}{2},n0\frac{1}{2}\frac{-1}{2}}(\mathbf{R})$
$(n,1,\frac{3}{2},\frac{3}{2})$	$(n,1,\frac{1}{2},\frac{1}{2})$	$e^{-i\frac{eB}{2\hbar}R_xR_y}\{t^{a_j,a_i}_{n1\frac{3}{2}\frac{3}{2},n1\frac{1}{2}\frac{1}{2}}(\mathbf{R})-\eta_\alpha t^{a_j,a_i}_{n1\frac{3}{2}\frac{3}{2},n1\frac{3}{2}\frac{1}{2}}(\mathbf{R})\}/\sqrt{1+\eta_\alpha^2}$
$(n,1,\frac{3}{2},\frac{3}{2})$	$(n,1,\frac{1}{2},-\frac{1}{2})$	$e^{-i\frac{eB}{2\hbar}R_xR_y}\{t^{a_j,a_i}_{n1\frac{3}{2}\frac{3}{2},n1\frac{1}{2}\frac{-1}{2}}(\mathbf{R})-\eta_\beta t^{a_j,a_i}_{n1\frac{3}{2}\frac{3}{2},n1\frac{3}{2}\frac{-1}{2}}(\mathbf{R})\}/\sqrt{1+\eta_\beta^2}$
$(n,1,\frac{3}{2},\frac{3}{2})$	$(n,1,\frac{3}{2},\frac{3}{2})$	$e^{-i\frac{eB}{2\hbar}R_xR_y}t^{a_j,a_i}_{n1\frac{3}{2}\frac{3}{2},n1\frac{3}{2}\frac{3}{2}}(\mathbf{R})$
$(n,1,\frac{3}{2},\frac{3}{2})$	$(n,1,\frac{3}{2},\frac{1}{2})$	$e^{-i\frac{eB}{2\hbar}R_xR_y}\{t^{a_j,a_i}_{n1\frac{3}{2}\frac{3}{2},n1\frac{3}{2}\frac{1}{2}}(\mathbf{R})+\eta_\alpha t^{a_j,a_i}_{n1\frac{3}{2}\frac{3}{2},n1\frac{1}{2}\frac{1}{2}}(\mathbf{R})\}/\sqrt{1+\eta_\alpha^2}$
$(n,1,\frac{3}{2},\frac{3}{2})$	$(n,1,\frac{3}{2},-\frac{1}{2})$	$e^{-i\frac{eB}{2\hbar}R_xR_y}\{t^{a_j,a_i}_{n1\frac{3}{2}\frac{3}{2},n1\frac{3}{2}\frac{-1}{2}}(\mathbf{R})+\eta_\beta t^{a_j,a_i}_{n1\frac{3}{2}\frac{3}{2},n1\frac{1}{2}\frac{-1}{2}}(\mathbf{R})\}/\sqrt{1+\eta_\beta^2}$
$(n,1,\frac{3}{2},\frac{3}{2})$	$(n,1,\frac{3}{2},-\frac{3}{2})$	$e^{-i\frac{eB}{2\hbar}R_xR_y}t^{a_j,a_i}_{n1\frac{3}{2}\frac{3}{2},n1\frac{3}{2}\frac{-3}{2}}(\mathbf{R})$
$(n,1,\frac{3}{2},\frac{1}{2})$	$(n,0,\frac{1}{2},\frac{1}{2})$	$e^{-i\frac{eB}{2\hbar}R_xR_y}\{t^{a_j,a_i}_{n1\frac{3}{2}\frac{1}{2},n0\frac{1}{2}\frac{1}{2}}(\mathbf{R})+\eta_\alpha t^{a_j,a_i}_{n1\frac{1}{2}\frac{1}{2},n0\frac{1}{2}\frac{1}{2}}(\mathbf{R})\}/\sqrt{1+\eta_\alpha^2}$
$(n,1,\frac{3}{2},\frac{1}{2})$	$(n,0,\frac{1}{2},-\frac{1}{2})$	$e^{-i\frac{eB}{2\hbar}R_xR_y}\{t^{a_j,a_i}_{n1\frac{3}{2}\frac{1}{2},n0\frac{1}{2}\frac{-1}{2}}(\mathbf{R})+\eta_\alpha t^{a_j,a_i}_{n1\frac{1}{2}\frac{1}{2},n0\frac{1}{2}\frac{-1}{2}}(\mathbf{R})\}/\sqrt{1+\eta_\alpha^2}$
$(n,1,\frac{3}{2},\frac{1}{2})$	$(n,1,\frac{1}{2},\frac{1}{2})$	$e^{-i\frac{eB}{2\hbar}R_xR_y}\{t^{a_j,a_i}_{n'1\frac{3}{2}\frac{1}{2},n1\frac{1}{2}\frac{1}{2}}(\mathbf{R})+\eta_\alpha t^{a_j,a_i}_{n'1\frac{1}{2}\frac{1}{2},n1\frac{1}{2}\frac{1}{2}}(\mathbf{R})$ $-\eta_\alpha t^{a_j,a_i}_{n'1\frac{3}{2}\frac{1}{2},n1\frac{3}{2}\frac{1}{2}}(\mathbf{R})-\eta_\alpha^2 t^{a_j,a_i}_{n'1\frac{1}{2}\frac{1}{2},n1\frac{3}{2}\frac{1}{2}}(\mathbf{R})\}/(1+\eta_\alpha^2)$
$(n,1,\frac{3}{2},\frac{1}{2})$	$(n,1,\frac{1}{2},-\frac{1}{2})$	$e^{-i\frac{eB}{2\hbar}R_xR_y}\{t^{a_j,a_i}_{n'1\frac{3}{2}\frac{1}{2},n1\frac{1}{2}\frac{-1}{2}}(\mathbf{R})+\eta_\alpha t^{a_j,a_i}_{n'1\frac{1}{2}\frac{1}{2},n1\frac{1}{2}\frac{-1}{2}}(\mathbf{R})$ $-\eta_\beta t^{a_j,a_i}_{n'1\frac{3}{2}\frac{1}{2},n1\frac{3}{2}\frac{-1}{2}}(\mathbf{R})-\eta_\alpha\eta_\beta t^{a_j,a_i}_{n'1\frac{1}{2}\frac{1}{2},n1\frac{3}{2}\frac{-1}{2}}(\mathbf{R})\}/\sqrt{(1+\eta_\alpha^2)(1+\eta_\beta^2)}$
$(n,1,\frac{3}{2},\frac{1}{2})$	$(n,1,\frac{3}{2},\frac{3}{2})$	$e^{-i\frac{eB}{2\hbar}R_xR_y}\{t^{a_j,a_i}_{n'1\frac{3}{2}\frac{1}{2},n1\frac{3}{2}\frac{3}{2}}(\mathbf{R})+\eta_\alpha t^{a_j,a_i}_{n'1\frac{1}{2}\frac{1}{2},n1\frac{3}{2}\frac{3}{2}}(\mathbf{R})\}/\sqrt{1+\eta_\alpha^2}$
$(n,1,\frac{3}{2},\frac{1}{2})$	$(n,1,\frac{3}{2},\frac{1}{2})$	$e^{-i\frac{eB}{2\hbar}R_xR_y}\{t^{a_j,a_i}_{n'1\frac{3}{2}\frac{1}{2},n1\frac{3}{2}\frac{1}{2}}(\mathbf{R})+\eta_\alpha t^{a_j,a_i}_{n'1\frac{1}{2}\frac{1}{2},n1\frac{3}{2}\frac{1}{2}}(\mathbf{R})$ $+\eta_\alpha t^{a_j,a_i}_{n'1\frac{3}{2}\frac{1}{2},n1\frac{1}{2}\frac{1}{2}}(\mathbf{R})+\eta_\alpha^2 t^{a_j,a_i}_{n'1\frac{1}{2}\frac{1}{2},n1\frac{1}{2}\frac{1}{2}}(\mathbf{R})\}/(1+\eta_\alpha^2)$
$(n,1,\frac{3}{2},\frac{1}{2})$	$(n,1,\frac{3}{2},-\frac{1}{2})$	$e^{-i\frac{eB}{2\hbar}R_xR_y}\{t^{a_j,a_i}_{n'1\frac{3}{2}\frac{1}{2},n1\frac{3}{2}\frac{-1}{2}}(\mathbf{R})+\eta_\alpha t^{a_j,a_i}_{n'1\frac{1}{2}\frac{1}{2},n1\frac{3}{2}\frac{-1}{2}}(\mathbf{R})$ $+\eta_\beta t^{a_j,a_i}_{n'1\frac{3}{2}\frac{1}{2},n1\frac{1}{2}\frac{-1}{2}}(\mathbf{R})+\eta_\alpha\eta_\beta t^{a_j,a_i}_{n'1\frac{1}{2}\frac{1}{2},n1\frac{1}{2}\frac{-1}{2}}(\mathbf{R})\}/\sqrt{(1+\eta_\alpha^2)(1+\eta_\beta^2)}$
$(n,1,\frac{3}{2},\frac{1}{2})$	$(n,1,\frac{3}{2},-\frac{3}{2})$	$e^{-i\frac{eB}{2\hbar}R_xR_y}\{t^{a_j,a_i}_{n'1\frac{3}{2}\frac{1}{2},n1\frac{3}{2}\frac{-3}{2}}(\mathbf{R})+\eta_\alpha t^{a_j,a_i}_{n'1\frac{1}{2}\frac{1}{2},n1\frac{3}{2}\frac{-3}{2}}(\mathbf{R})\}/\sqrt{1+\eta_\alpha^2}$

TABLE I. (*Continued*.)

(n,l',J',M')	(n,l,J,M)	Hopping integrals $T^{a_j,a_i}_{nl'J'M',nlJM}(\mathbf{R})$
$(n,1,\frac{3}{2},-\frac{1}{2})$	$(n,0,\frac{1}{2},\frac{1}{2})$	$e^{-i\frac{eB}{2\hbar}R_xR_y}\{t^{a_j,a_i}_{n'1\frac{3}{2}\frac{-1}{2},n0\frac{1}{2}\frac{1}{2}}(\mathbf{R})+\eta_\beta t^{a_j,a_i}_{n'1\frac{1}{2}\frac{-1}{2},n0\frac{1}{2}\frac{1}{2}}(\mathbf{R})\}/\sqrt{1+\eta_\beta^2}$
$(n,1,\frac{3}{2},-\frac{1}{2})$	$(n,0,\frac{1}{2},-\frac{1}{2})$	$e^{-i\frac{eB}{2\hbar}R_xR_y}\{t^{a_j,a_i}_{n'1\frac{3}{2}\frac{-1}{2},n0\frac{1}{2}\frac{-1}{2}}(\mathbf{R})+\eta_\beta t^{a_j,a_i}_{n'1\frac{1}{2}\frac{-1}{2},n0\frac{1}{2}\frac{-1}{2}}(\mathbf{R})\}/\sqrt{1+\eta_\beta^2}$
$(n,1,\frac{3}{2},-\frac{1}{2})$	$(n,1,\frac{1}{2},\frac{1}{2})$	$e^{-i\frac{eB}{2\hbar}R_xR_y}\{t^{a_j,a_i}_{n'1\frac{3}{2}\frac{-1}{2},n1\frac{1}{2}\frac{1}{2}}(\mathbf{R})+\eta_\beta t^{a_j,a_i}_{n'1\frac{1}{2}\frac{-1}{2},n1\frac{1}{2}\frac{1}{2}}(\mathbf{R})$ $-\eta_\alpha t^{a_j,a_i}_{n'1\frac{3}{2}\frac{-1}{2},n1\frac{3}{2}\frac{1}{2}}(\mathbf{R})-\eta_\alpha\eta_\beta t^{a_j,a_i}_{n'1\frac{1}{2}\frac{-1}{2},n1\frac{3}{2}\frac{1}{2}}(\mathbf{R})\}/\sqrt{(1+\eta_\alpha^2)(1+\eta_\beta^2)}$
$(n,1,\frac{3}{2},-\frac{1}{2})$	$(n,1,\frac{1}{2},-\frac{1}{2})$	$e^{-i\frac{eB}{2\hbar}R_xR_y}\{t^{a_j,a_i}_{n'1\frac{3}{2}\frac{-1}{2},n1\frac{1}{2}\frac{-1}{2}}(\mathbf{R})+\eta_\beta t^{a_j,a_i}_{n'1\frac{1}{2}\frac{-1}{2},n1\frac{1}{2}\frac{-1}{2}}(\mathbf{R})$ $-\eta_\beta t^{a_j,a_i}_{n'1\frac{3}{2}\frac{-1}{2},n1\frac{3}{2}\frac{-1}{2}}(\mathbf{R})-\eta_\beta^2 t^{a_j,a_i}_{n'1\frac{1}{2}\frac{-1}{2},n1\frac{3}{2}\frac{-1}{2}}(\mathbf{R})\}/(1+\eta_\beta^2)$
$(n,1,\frac{3}{2},-\frac{1}{2})$	$(n,1,\frac{3}{2},\frac{3}{2})$	$e^{-i\frac{eB}{2\hbar}R_xR_y}\{t^{a_j,a_i}_{n'1\frac{3}{2}\frac{-1}{2},n1\frac{3}{2}\frac{3}{2}}(\mathbf{R})+\eta_\beta t^{a_j,a_i}_{n'1\frac{1}{2}\frac{-1}{2},n1\frac{3}{2}\frac{3}{2}}(\mathbf{R})\}/\sqrt{1+\eta_\beta^2}$
$(n,1,\frac{3}{2},-\frac{1}{2})$	$(n,1,\frac{3}{2},\frac{1}{2})$	$e^{-i\frac{eB}{2\hbar}R_xR_y}\{t^{a_j,a_i}_{n'1\frac{3}{2}\frac{-1}{2},n1\frac{3}{2}\frac{1}{2}}(\mathbf{R})+\eta_\beta t^{a_j,a_i}_{n'1\frac{1}{2}\frac{-1}{2},n1\frac{3}{2}\frac{1}{2}}(\mathbf{R})$ $+\eta_\alpha t^{a_j,a_i}_{n'1\frac{3}{2}\frac{-1}{2},n1\frac{1}{2}\frac{1}{2}}(\mathbf{R})+\eta_\alpha\eta_\beta t^{a_j,a_i}_{n'1\frac{1}{2}\frac{-1}{2},n1\frac{1}{2}\frac{1}{2}}(\mathbf{R})\}/\sqrt{(1+\eta_\alpha^2)(1+\eta_\beta^2)}$
$(n,1,\frac{3}{2},-\frac{1}{2})$	$(n,1,\frac{3}{2},-\frac{1}{2})$	$e^{-i\frac{eB}{2\hbar}R_xR_y}\{t^{a_j,a_i}_{n'1\frac{3}{2}\frac{-1}{2},n1\frac{3}{2}\frac{-1}{2}}(\mathbf{R})+\eta_\beta t^{a_j,a_i}_{n'1\frac{1}{2}\frac{-1}{2},n1\frac{3}{2}\frac{-1}{2}}(\mathbf{R})$ $+\eta_\beta t^{a_j,a_i}_{n'1\frac{3}{2}\frac{-1}{2},n1\frac{1}{2}\frac{-1}{2}}(\mathbf{R})+\eta_\beta^2 t^{a_j,a_i}_{n'1\frac{1}{2}\frac{-1}{2},n1\frac{1}{2}\frac{-1}{2}}(\mathbf{R})\}/(1+\eta_\beta^2)$
$(n,1,\frac{3}{2},-\frac{1}{2})$	$(n,1,\frac{3}{2},-\frac{3}{2})$	$e^{-i\frac{eB}{2\hbar}R_xR_y}\{t^{a_j,a_i}_{n'1\frac{3}{2}\frac{-1}{2},n1\frac{3}{2}\frac{-3}{2}}(\mathbf{R})+\eta_\beta t^{a_j,a_i}_{n'1\frac{1}{2}\frac{-1}{2},n1\frac{3}{2}\frac{-3}{2}}(\mathbf{R})\}/\sqrt{1+\eta_\beta^2}$
$(n,1,\frac{3}{2},-\frac{3}{2})$	$(n,0,\frac{1}{2},\frac{1}{2})$	$e^{-i\frac{eB}{2\hbar}R_xR_y}t^{a_j,a_i}_{n'1\frac{3}{2}\frac{-3}{2},n0\frac{1}{2}\frac{1}{2}}(\mathbf{R})$
$(n,1,\frac{3}{2},-\frac{3}{2})$	$(n,0,\frac{1}{2},-\frac{1}{2})$	$e^{-i\frac{eB}{2\hbar}R_xR_y}t^{a_j,a_i}_{n'1\frac{3}{2}\frac{-3}{2},n'0\frac{1}{2}\frac{-1}{2}}(\mathbf{R})$
$(n,1,\frac{3}{2},-\frac{3}{2})$	$(n,1,\frac{1}{2},\frac{1}{2})$	$e^{-i\frac{eB}{2\hbar}R_xR_y}\{t^{a_j,a_i}_{n'1\frac{3}{2}\frac{-3}{2},n1\frac{1}{2}\frac{1}{2}}(\mathbf{R})-\eta_\alpha t^{a_j,a_i}_{n'1\frac{3}{2}\frac{-3}{2},n1\frac{3}{2}\frac{1}{2}}(\mathbf{R})\}/\sqrt{1+\eta_\alpha^2}$
$(n,1,\frac{3}{2},-\frac{3}{2})$	$(n,1,\frac{1}{2},-\frac{1}{2})$	$e^{-i\frac{eB}{2\hbar}R_xR_y}\{t^{a_j,a_i}_{n'1\frac{3}{2}\frac{-3}{2},n1\frac{1}{2}\frac{-1}{2}}(\mathbf{R})-\eta_\beta t^{a_j,a_i}_{n'1\frac{3}{2}\frac{-3}{2},n1\frac{3}{2}\frac{-1}{2}}(\mathbf{R})\}/\sqrt{1+\eta_\beta^2}$
$(n,1,\frac{3}{2},-\frac{3}{2})$	$(n,1,\frac{3}{2},\frac{3}{2})$	$e^{-i\frac{eB}{2\hbar}R_xR_y}t^{a_j,a_i}_{n'1\frac{3}{2}\frac{-3}{2},n1\frac{3}{2}\frac{3}{2}}(\mathbf{R})$
$(n,1,\frac{3}{2},-\frac{3}{2})$	$(n,1,\frac{3}{2},\frac{1}{2})$	$e^{-i\frac{eB}{2\hbar}R_xR_y}\{t^{a_j,a_i}_{n'1\frac{3}{2}\frac{-3}{2},n1\frac{3}{2}\frac{1}{2}}(\mathbf{R})+\eta_\alpha t^{a_j,a_i}_{n'1\frac{3}{2}\frac{-3}{2},n1\frac{1}{2}\frac{1}{2}}(\mathbf{R})\}/\sqrt{1+\eta_\alpha^2}$
$(n,1,\frac{3}{2},-\frac{3}{2})$	$(n,1,\frac{3}{2},-\frac{1}{2})$	$e^{-i\frac{eB}{2\hbar}R_xR_y}\{t^{a_j,a_i}_{n'1\frac{3}{2}\frac{-3}{2},n1\frac{3}{2}\frac{-1}{2}}(\mathbf{R})+\eta_\beta t^{a_j,a_i}_{n'1\frac{3}{2}\frac{-3}{2},n1\frac{1}{2}\frac{-1}{2}}(\mathbf{R})\}/\sqrt{1+\eta_\beta^2}$
$(n,1,\frac{3}{2},-\frac{3}{2})$	$(n,1,\frac{3}{2},-\frac{3}{2})$	$e^{-i\frac{eB}{2\hbar}R_xR_y}t^{a_j,a_i}_{n'1\frac{3}{2}\frac{-3}{2},n1\frac{3}{2}\frac{-3}{2}}(\mathbf{R})$

effect (low magnetic field case) but also the Paschen-Back effect (high magnetic field case).

IV. APPLICATION OF THE EXT-MFRTB METHOD TO THE CRYSTALLINE SILICON IMMERSED IN A MAGNETIC FIELD

In order to confirm the validity of the ext-MFRTB method, we apply this method to the crystalline silicon immersed in a magnetic field. Eigenvalues are calculated by diagonalizing the Hamiltonian matrix Eq. (2) by taking into account the magnetic Bloch theorem [18]. In the calculation, we take into consideration magnetic hopping integrals between the outermost shells of the nearest-neighbor atoms. Namely, atomic orbitals with $(n,l,J,M) = (3,0,1/2,\pm 1/2)$, $(3,1,1/2,\pm 1/2)$, $(3,1,3/2,\pm 1/2)$, and $(3,1,3/2,\pm 3/2)$ are considered. With respect to the tight-binding parameters of the crystalline silicon for the zero-magnetic-field case, we adopt the same ones used in the previous paper [18]. We suppose that the magnetic field is parallel to the c axis and its magnitude is given by

$$B = \frac{16\pi\hbar}{ea^2}\frac{p}{q}, \tag{15}$$

where a (=0.543 nm) denotes the lattice constant, and p and q are relatively prime integers [18]. Substituting the value of a into this expression, we have $B = 1.122\times 10^5(p/q)$ T. Therefore, the value of p/q that yields $x_{nl} = 1$ is about 0.00454.

The butterfly diagrams are obtained by calculating the magnetic field dependence of eigenvalues that are associated with wave vectors lying in the k_x-k_y plane of the magnetic first Brillouin zone [18]. We calculate four kinds of butterfly diagrams. (a) One [Fig. 1(a)] is calculated by the MFRTB method with neglecting the Zeeman term of Eq. (8). Namely, the butterfly diagram obtained by this method corresponds to the original Hofstadter butterfly diagram. (b) The second one

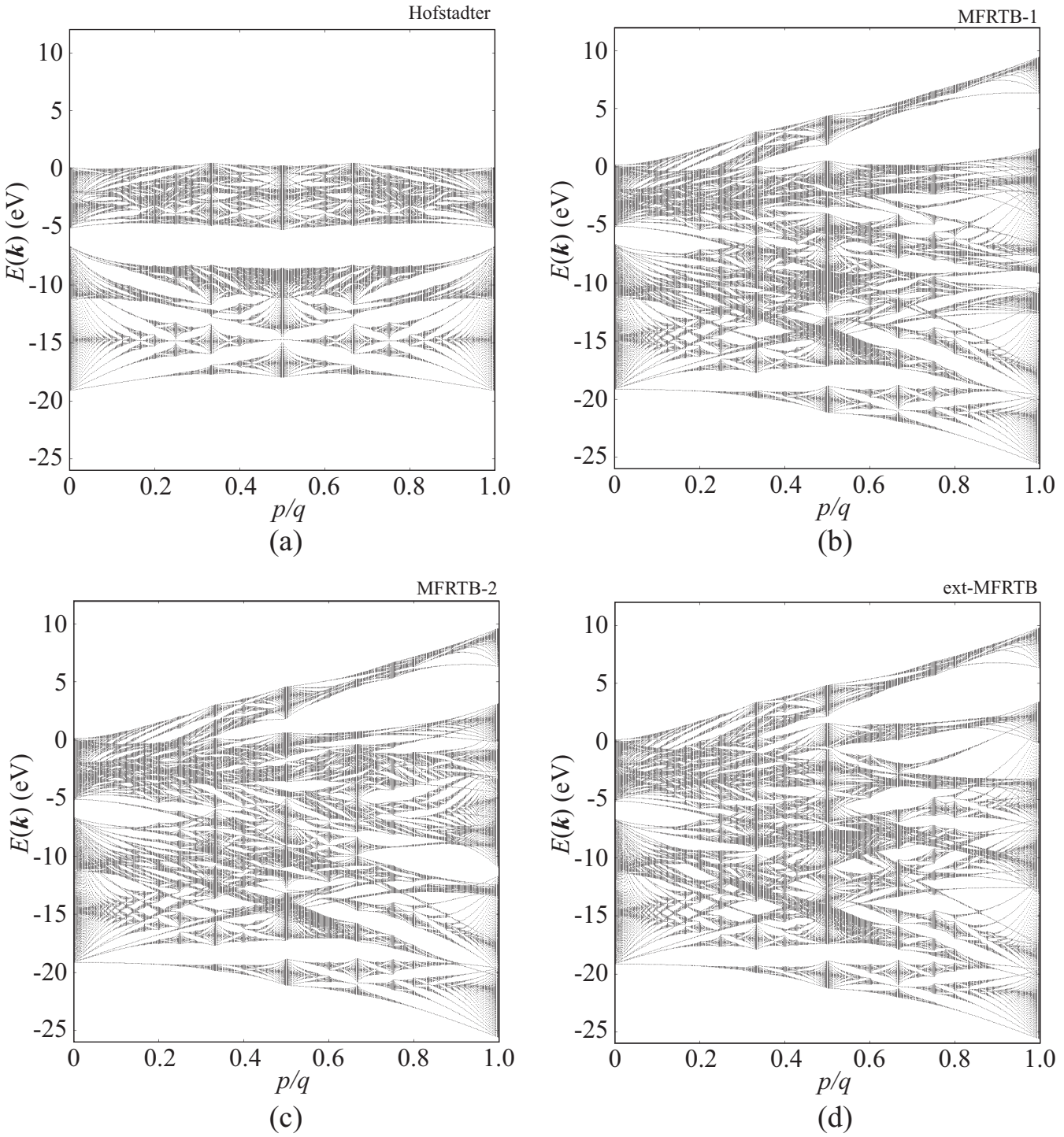

FIG. 1. Butterfly diagrams calculated by the (a) Hofstadter method, (b) MFRTB method 1, (c) MFRTB method 2, and (d) ext-MFRTB. These four calculation methods are summarized in Table II.

[Fig. 1(b)] is calculated by the MFRTB method. (c) The third one [Fig. 1(c)] is calculated by using Eqs. (10) and (13) as the atomic spectrum instead of Eq. (8). The difference between Fig. 1(b) and Fig. 1(c) comes from the different treatment of the atomic spectrum. (d) The fourth one [Fig. 1(d)] is calculated by the present method (ext-MFRTB method), i.e., by using Eqs. (10) and (13) as the atomic spectrum, and by using Table I in calculating magnetic hopping integrals. Note that the difference between Fig. 1(c) and Fig. 1(d) comes from the different treatment of the magnetic hopping integral. For convenience, these calculation methods are summarized in Table II.

In the low magnetic field (low p/q) limit, the energy gap appears around -6 eV for all butterfly diagrams [Figs. 1(a)–1(d)]. This gap corresponds to the original energy band gap of the crystalline silicon. Comparing Fig. 1(a) with Fig. 1(b),

TABLE II. Calculation methods performed in this study.

	Atomic spectrum	Magnetic hopping integral
(a) Hofstadter method	$\bar{\varepsilon}^{a_i}_{nlJ}$	Eq. (9)
(b) MFRTB method 1	Eq. (8)	Eq. (9)
(c) MFRTB method 2	Eqs. (10) and (13)	Eq. (9)
(d) ext-MFRTB method	Eqs. (10) and (13)	Table I

the butterfly diagram in Fig. 1(b) increases or decreases with the magnetic field due to the Zeeman term [the second term of Eq. (8)].

Figure 1(c) is similar to Fig. 1(b) in the low magnetic field region. This is because Eq. (8) is close to Eq. (10) or Eq. (13) in the low magnetic field region, as shown in Fig. 2. It is also found from Fig. 1(b) and Fig. 1(c) that the butterfly diagram in the higher- (>0 eV) and lower-energy ranges (<-15 eV) of Fig. 1(b) are similar to those of Fig. 1(c) even in the high magnetic field region. This implies that the eigenstates with the higher and lower energies contain atomic states of $(n,l,J,M)=(3,1,3/2,\pm 3/2)$,$(3,0,1/2,\pm 1/2)$, with relatively high weight because Eq. (8) is identical with Eq. (13) for these atomic states. On the other hand, the discrepancy between the butterfly diagrams of Fig. 1(b) and Fig. 1(c) becomes clear in the middle-energy range at the high magnetic field region. This is because Eq. (10) with $(n,l,J,M)=(3,1,3/2,-1/2)$ and $(3,1,1/2,1/2)$ approaches zero with increasing magnetic field, while Eq. (8) incorrectly decreases or increases with the magnetic field (Fig. 2). Due to this correction, the discrepancy between Fig. 1(b) and Fig. 1(c) becomes clear in the middle-energy range at the high magnetic field region.

It is found that the butterfly diagram of Fig. 1(d) approaches that of Fig. 1(c) in the low magnetic field limit. This is because the mixing coefficient $\eta^{a_i}_{nlJM}$ approaches zero in the low magnetic field limit (Fig. 3), so that the magnetic hopping integrals listed in Table I approach the conventional approximation form Eq. (9). The mixing coefficient rapidly increases with the magnetic field as shown in Fig. 3. Therefore, the discrepancy between Fig. 1(d) and Fig. 1(c) becomes clear not only in the high magnetic field region but also in the low magnetic field region.

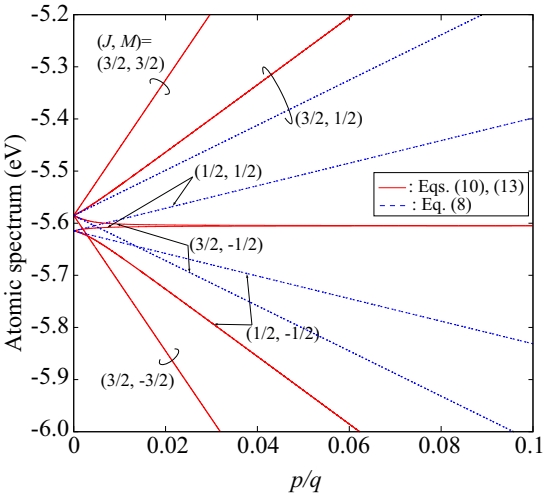

FIG. 2. Magnetic field dependencies of atomic spectra for $(n,l,J,M)=(3,1,1/2,\pm 1/2)$, $(3,1,3/2,\pm 1/2)$, and $(3,1,3/2,\pm 3/2)$. These are calculated by using Eq. (8) (blue dashed lines) and by using Eqs. (10) and (13) (red solid lines).

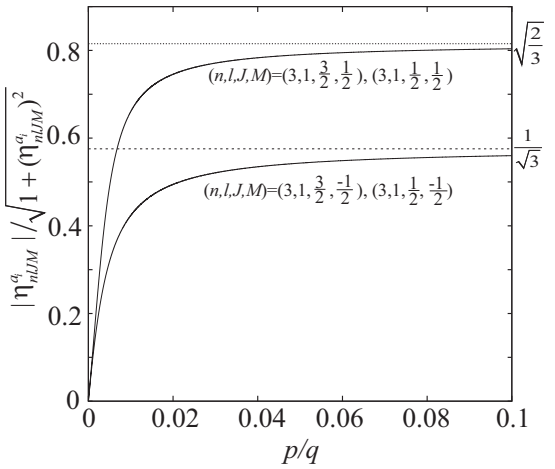

FIG. 3. Magnetic field dependencies of the normalized mixing coefficient $|\eta^{a_i}_{nlJM}|/\sqrt{1+(\eta^{a_i}_{nlJM})^2}$. In the high magnetic field, the relativistic atomic orbitals in the presence of a magnetic field approach simultaneous eigenfunctions of z components of the orbital and spin angular momentums, which is known as the Paschen-Back effect [30]. Corresponding to this, the normalized mixing coefficients approach constant values ($\sqrt{2/3}$ or $1/\sqrt{3}$) as shown in the figure.

Figures 4(a)–4(d) are the magnified views of Figs. 1(a)–1(d) around the energy gap, respectively. The range of the horizontal axis of these figures is set from 0 to 0.005. Since the value of p/q that yields $x_{nl}=1$ is about 0.00454, we can check the superiority of the present method over previous ones more strictly in this range. It is found that magnetic field dependencies of unoccupied energy levels (upper side) shown in Fig. 4(a) are very different from those shown in Figs. 4(b)–4(d) due to magnetic field dependencies of atomic spectra. On the other hand, magnetic field dependencies of unoccupied energy levels shown in Figs. 4(b)–4(d) are similar to each other. This means that the Paschen-Back effect does not clearly appear in the unoccupied energy levels for the crystalline silicon. This would be because these unoccupied energy states do not contain too much atomic states of $(n,l,J,M)=(3,1,3/2,\pm 1/2)$ and $(3,1,1/2,\pm 1/2)$ that are mixed through the Paschen-Back effect [Eq. (11)].

Similarly to the unoccupied energy levels, the magnetic field dependencies of occupied energy levels (lower side) shown in Fig. 4(a) are very different from those in Figs. 4(b)–4(d), which suggests that the magnetic field dependence of the atomic spectrum should be taken into consideration. It is also found that the occupied energy levels are much revised by using Table I as the approximate forms of magnetic hopping integrals. Namely, although occupied energy levels shown in Fig. 4(b) are similar to those in Fig. 4(c), they are very different from those in Fig. 4(d). Specifically, the second and third energy levels cross at around $p/q=0.002$ ($B\sim 224$ T) in Fig. 4(d), while those

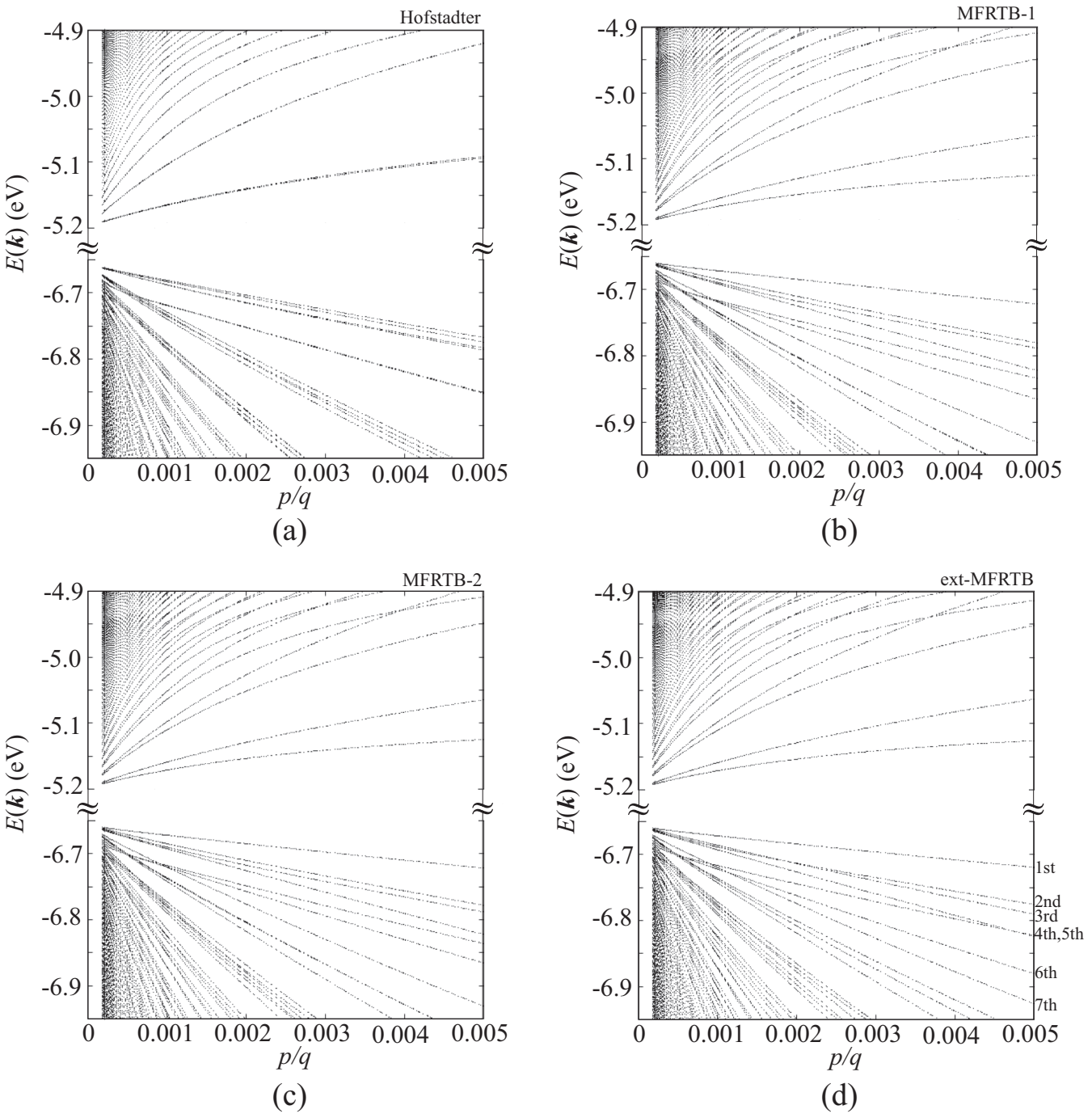

FIG. 4. Butterfly diagrams around the energy gap. (a), (b), (c), and (d) are magnified views of Figs. 1(a)–1(d) (Hofstadter, MFRTB 1, MFRTB 2, and ext-MFRTB), respectively. The range of the horizontal axis corresponds to $0 \leqslant B \leqslant 561$ T.

in Figs. 4(b) and 4(c) do not cross. In addition, the 5th–7th energy levels shown in Fig. 4(d) cross at around $p/q = 0.001$ ($B \sim 112$ T) in a different way from those in Figs. 4(b) and 4(c). Since the magnetic hopping integrals listed in Table I are obtained by incorporating the Paschen-Back effect into the magnetic hopping integral as mentioned in Sec. III, these characteristic differences are regarded as the emergence of the Paschen-Back effect in the butterfly diagram of the crystalline silicon. Thus, the Pashen-Back effect in crystalline silicon is expected to be observed in ultrahigh magnetic field ranging from 100 T to 250 T that is experimentally available [24–27].

V. CONCLUDING REMARKS

We develop the first-principles calculation method (ext-MFRTB method) for materials immersed in a magnetic field on the basis of the nonperturbative theory. Due to the nonperturbative method, both the Zeeman effect and Paschen-Back

effect are taken into consideration in calculating the electronic structure of materials immersed in a magnetic field. The most striking feature of the present method is that we can obtain the butterfly diagram of energy spectra that is valid for not only the low magnetic field region but also the high magnetic field region.

We apply the present method to the crystalline silicon immersed in a magnetic field. It is found that the conventional Hofstadter butterfly diagram is corrected by means of the present method not only in the high magnetic field region but also in the low magnetic field region. Specifically, the present method predicts the energy-level crossing of occupied states, which is regarded as the emergence of the Paschen-Back effect in the butterfly diagram of the crystalline silicon. This effect may be observed experimentally. For example, a quantum-well structure immersed in a magnetic field perpendicular to the well layer, such as SiO/Si/SiO and SiC/Si/SiC heterostructures immersed in a magnetic field, seems to be one of the possible systems.

ACKNOWLEDGMENTS

This work was supported by JSPS KAKENHI Grants No. JP26400354, No. JP26400397, and No. JP16H00916.

[1] D. Hofstadter, Phys. Rev. B **14**, 2239 (1976).
[2] D. J. Thouless, M. Kohmoto, M. P. Nightingale, and M. den Nijs, Phys. Rev. Lett. **49**, 405 (1982).
[3] P. Středa, J. Phys. C **15**, L1299 (1982).
[4] A. H. MacDonald, Phys. Rev. B **28**, 6713 (1983).
[5] K. Machida, K. Kishigi, and Y. Hori, Phys. Rev. B **51**, 8946 (1995).
[6] S. Y. Han, J. S. Brooks, and J. H. Kim, Phys. Rev. Lett. **85**, 1500 (2000).
[7] K. Kishigi and Y. Hasegawa, Phys. Rev. B **65**, 205405 (2002).
[8] O. Gat and J. E. Avron, Phys. Rev. Lett. **91**, 186801 (2003).
[9] M. Taut, H. Eschrig, and M. Richter, Phys. Rev. B **72**, 165304 (2005).
[10] V. M. Gvozdikov and M. Taut, Phys. Rev. B **75**, 155436 (2007).
[11] W. H. Xu, L. P. Yang, M. P. Qin, and T. Xiang, Phys. Rev. B **78**, 241102(R) (2008).
[12] K. Kishigi and Y. Hasegawa, Phys. Rev. B **90**, 085427 (2014).
[13] C. Albrecht, J. H. Smet, K. von Klitzing, D. Weiss, V. Umansky, and H. Schweizer, Phys. Rev. Lett. **86**, 147 (2001).
[14] M. C. Geisler, J. H. Smet, V. Umansky, K. von Klitzing, B. Naundorf, R. Ketzmerick, and H. Schweizer, Phys. Rev. Lett. **92**, 256801 (2004).
[15] L. A. Ponomarenko, R. V. Gorbachev, G. L. Yu, D. C. Elias, R. Jalil, A. A. Patel, A. Mishchenko, A. S. Mayorov, C. R. Woods, J. R. Wallbank, M. Mucha-Kruczynski, B. A. Piot, M. Potemski, I. V. Grigorieva, K. S. Novoselov, F. Guinea, V. I. Falko, and A. K. Geim, Nature (London) **497**, 594 (2013).
[16] C. Dean, L. Wang, P. Maher, C. Forsythe, F. Ghahari, Y. Gao, J. Katoch, M. Ishigami, P. Moon, M. Koshino, T. Taniguchi, K. Watanabe, K. Shepard, J. Hone, and P. Kim, Nature (London) **497**, 598 (2013).
[17] G. L. Yu, R. V. Gorbachev, J. S. Tu, A. V. Kretinin, Y. Cao, R. Jalil, F. Withers, L. A. Ponomarenko, B. A. Piot, M. Potemski, D. C. Elias, X. Chen, K. Watanabe, T. Taniguchi, I. V. Grigorieva, K. S. Novoselov, V. I. Falko, A. K. Geim, and A. Mishchenko, Nat. Phys. **10**, 525 (2014).
[18] K. Higuchi, D. B. Hamal, and M. Higuchi, Phys. Rev. B **91**, 075122 (2015).
[19] D. B. Hamal, M. Higuchi, and K. Higuchi, Phys. Rev. B **91**, 245101 (2015).
[20] M. Higuchi, D. Bahadur Hamal, and K. Higuchi, Phys. Rev. B **95**, 195153 (2017).
[21] K. Higuchi, D. B. Hamal, and M. Higuchi, Phys. Rev. B **96**, 235125 (2017).
[22] I. M. Lifshitz and A. M. Kosevich, Sov. Phys. JETP **2**, 636 (1956).
[23] M. P. Marder, *Condensed Matter Physics* (Wiley, New York, 2000), Chap. 25.
[24] S. Takeyama and E. Kojima, J. Phys. D: Appl. Phys. **44**, 425003 (2011).
[25] D. Nakamura, Y. H. Matsuda, and S. Takeyama, J. Low Temp. Phys. **170**, 457 (2013).
[26] D. Nakamura, T. Sasaki, W. Zhou, H. Liu, H. Kataura, and S. Takeyama, Phys. Rev. B **91**, 235427 (2015).
[27] A. Miyata, H. Ueda, Y. Ueda, H. Sawabe, and S. Takeyama, Phys. Rev. Lett. **107**, 207203 (2011).
[28] These values of spin-orbit splitting are obtained by the density functional calculations.
[29] A. Messiah, *Quantum Mechanics* (North-Holland, Amsterdam, 1966), Chap. 20.
[30] H. Friedrich, *Theoretical Atomic Physics*, 3rd ed. (Springer, Berlin, 2006), Chap. 3.